Frontiers of Optoelectronics (2022) 15:20
https://doi.org/10.1007/s12200-022-00023-6

Frontiers of Optoelectronics

RESEARCH ARTICLE

Complete photonic bandgap in silicon nitride slab assisted by effective index difference between polarizations

Can Ma[1] · Jin Hou[1] · Chunyong Yang[1] · Ming Shi[1] · Shaoping Chen[1]

Received: 21 June 2021 / Accepted: 7 September 2021

Abstract
The slab effective index difference between the transverse-electric (TE) and transverse-magnetic (TM) polarizations was utilized to obtain complete photonic bandgap (CPBG) in a silicon nitride (Si_xN_y) photonic crystal slab. For this, coincident frequency range in the TE photonic bandgap (PBG) and TM PBG, which denotes the CPBGs of the slab, must be found with the same structure. Through adjusting the effective index pair of TE and TM polarizations by changing the thickness of the Si_xN_y core layer, and also optimizing the structure parameters within the photonic crystal plane, a large normalized CPBG of 5.62% was theoretically obtained in a slab of Si_xN_y with a refractive index of 2.5. Moreover, based on the obtained CPBG, a microcavity which could support both TE and TM polarization was theoretically demonstrated. The cavity modes for different polarizations were both well confined, which proved the reliability of the CPBG. In addition, using the same method, the lowest refractive index of Si_xN_y on silica slab for a CPBG could be extended to as low as 2. The results indicate that there is potential for development of various high-performance CPBG devices based on Si_xN_y slab technology.

Keywords Silicon nitride slab · Complete photonic bandgap (CPBG) · Microcavity · Slab device

1 Introduction

Because of the small mode volumes and high quality factors [1], silicon-based photonic bandgap (PBG) devices have been regarded as the essential elements for miniaturization and integration [2]. Compared with PBG for one single polarization, the complete photonic bandgap (CPBG), which has PBGs for both transverse-electric (TE) and transverse-magnetic (TM) polarizations, is of particular interest for reduced loss of light propagation [3] and the ability to polarize multiplex [4]. Therefore, various powerful silicon photonic devices based on CPBG have been demonstrated theoretically and experimentally, such as high-Q microcavity [1], polarization beam splitter [2, 5, 6], polarization-independent waveguide [7, 8], etc. However, currently most of these devices are based on the SOI platform which has a high refractive index contrast (RIC) [2, 3, 5–9]. Unfortunately, bulk crystalline silicon has non-negligible two-photon absorption [10] in all telecommunication bands with wavelengths shorter than about 2000 nm, which seriously affects the efficiency of nonlinear photonic chips in generating and processing all-optical signals [11, 12]. Therefore, some new platforms compatible with CMOS processes, such as silicon nitride (Si_xN_y), Hydex, have been proposed previously [11]. But the RICs of these new material platforms are lower than that of SOI, which makes them difficult to obtain CPBGs. In other words, although the proposal of the new platforms relieves the problem of non-negligible two-photon absorption in crystalline silicon, they cannot inherit the advantage of the easy access to CPBG that is provided by the SOI platform. Therefore, obtaining the CPBG under relatively low RICs corresponding to the new platforms remains a problem.

Many efforts have been made in the past few years to obtain a CPBG at lower RICs [13–15]. By rotation angle, a hexagonal air hole structure based on rutile TiO_2 with a refractive index of 2.85 has been proposed and a CPBG of 1.5% has been obtained [14]. Moreover, chalcogenide photonic crystal (PC) slow light waveguides with RICs of 2.85 and 2.6 have been reported respectively [15, 16]. Through

✉ Jin Hou
houjin@mail.scuec.edu.cn

[1] Hubei Key Laboratory of Intelligent Wireless Communications, Hubei Engineering Research Center for Intelligent Internet of Things, College of Electronic and Information Engineering, South-Central MinZu University, Wuhan 430074, China

Published online: 06 May 2022

focused ion beam milling technology, highly efficient evanescent coupling between a chalcogenide glass PC waveguide with RIC of 2.7 and a silica fiber nanowire has been demonstrated [17]. Furthermore, by suitably designed supercell PCs, when the RIC is 2.57 corresponding to diamond and strontium titanate, a hexagonal connecting-rods PC slab has been found to be able to support a CPBG of 5.6% [18]. In summary, CPBGs could potentially be obtained in slabs with moderate RIC material platforms, such as rutile TiO_2, strontium titanate, diamond and chalcogenide glasses. However, to the best of our knowledge, there is no report about CPBG in a Si_xN_y slab. The transparent window of Si_xN_y can be extended from infrared to the visible light band [19]. Moreover, because of the high-quality CMOS-compatible fabrication processes, and of the negligible two-photon absorption at telecommunication wavelengths, Si_xN_y platform technology is particularly promising [12]. Since the x and y parameters in Si_xN_y are adjustable, the refractive index of Si_xN_y also can be varied between 2 and 3.1 [11, 20, 21]. Therefore, in this work, CPBG in a PC slab with the Si_xN_y index within 2–2.5 was engineered, making use of the slab effective index [22–24] difference between TE polarization and TM polarization, and which could be adjusted by the slab thickness.

2 Scheme and structure

In 2D ideal PCs, the lowest RIC for TM PBG is usually lower than that for TE PBG; the lowest RIC for a CPBG is therefore restricted by that for a TE PBG. Accordingly, it has been widely thought that, when the slab effective index is lower than the lowest RIC for a TE PBG of its corresponding 2D type, it is difficult to obtain CPBG in a slab type PC. Fortunately, in a sandwiched slab structure like Si_xN_y on silica cladding, the slab effective index for TM polarization is usually lower than that for TE polarization, as shown in Fig. 1a. Thus, utilizing the lower slab effective index of TM polarization, and also considering the lowest RIC for TM PBG in 2D ideal PCs is lower than that for TE PBG [18, 25], it is possible to have a TM PBG with an effective index lower than that for a TE polarization. Therefore, if the coincident frequency range in the TE PBGs and TM PBGs could be found with the same structure parameters and with their corresponding effective indices for the two polarizations, obtaining CPBGs of a slab with effective index for TM polarization lower than that for TE polarization is possible, as illustrated in Fig. 1b.

The detail of the scheme to obtain CPBG in a Si_xN_y PC slab by utilizing the effective index difference between polarizations is shown in Fig. 1. In Fig. 1a, a typical example of the effective indices for the lowest two guided polarization modes in a Si_xN_y slab is shown. The right lower inset of Fig. 1a shows a schematic structure of Si_xN_y slab, in which a Si_xN_y guided layer with a refractive index of 2.5 is sandwiched between a silica sub-cladding layer and an air upper-cladding layer. The thickness of the Si_xN_y guided layer (represented by b), corresponding to each frequency at 1.55 μm wavelength, is also shown. Here, the effective indices for the lowest two guided polarization modes in a Si_xN_y slab were obtained by considering the light confinement in a vertical dimension (z direction) with a 1D method [23]. The effective

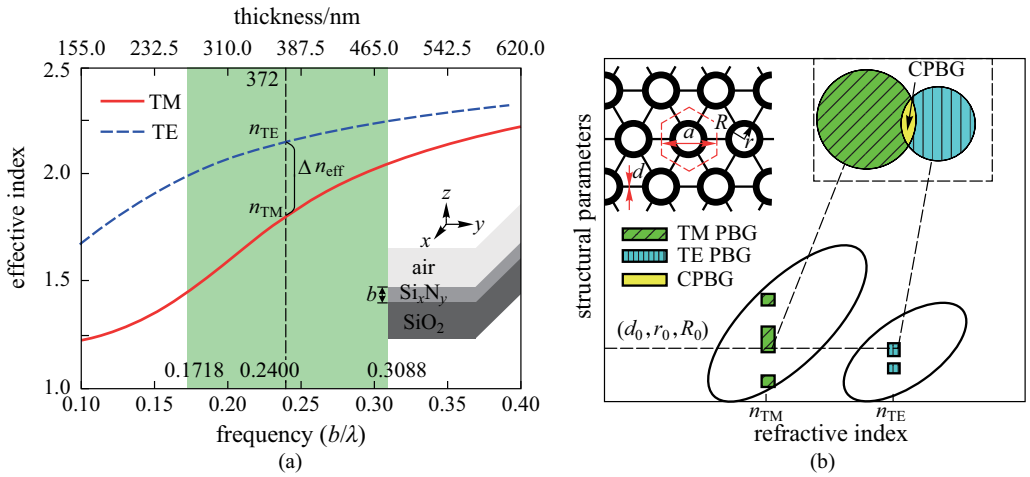

Fig. 1 **a** Effective indices of TE and TM polarizations with different frequencies in a Si_xN_y slab, green shadow denotes the single-mode range, and the right lower inset shows a schematic structure of the slab, in which b represents the thickness of the Si_xN_y guided layer. The lower axis represents the frequency, and the upper axis represents the corresponding thickness of the Si_xN_y guided layer at the fixed wavelength of 1.55 μm. **b** Schematic diagram of obtaining CPBG in a Si_xN_y PC slab by utilizing the effective index difference between polarizations. The left upper inset shows a schematic structure of the connecting annular holes PC (CAPC) proposed in this paper, in which the black color represents Si_xN_y and the white color represents air

indices and the photonic band structures in this paper were all calculated with the MPB software developed by MIT, which casts the Maxwell equations as a Hermitian eigenvalue problem with the plane wave expansion technique [26].

In Fig. 1a, one may easily find that the effective index of TM polarization (denoted as n_{TM}) is lower than that of TE polarization (denoted as n_{TE}) at the same wavelength or frequency. And at the same wavelength or frequency, the n_{TE} and n_{TM} are a pair, corresponding to each other. Between normalized frequencies 0.1718 and 0.3088 (b/λ), we confirmed that both TE and TM polarizations are single mode. It means that within the single mode frequency range denoted as green, there is usually a nonzero Δn_{eff} between n_{TE} and n_{TM}. Meanwhile, as shown in Fig. 1b, using the corresponding pair of effective indices found in Fig. 1a, TM PBGs and TE PBGs can be obtained with different structural parameter ranges represented by the green slash areas and the blue vertical line areas, respectively. Thus, if the overlapped frequency range of the TE PBGs and TM PBGs can be found under the same structural parameter, marked as (d_0, r_0, R_0), CPBG in a PC slab can be obtained, as shown in the yellow area of Fig. 1b. In other words, CPBG in a Si_xN_y PC slab with low RIC can be obtained.

The key point for obtaining the CPBGs becomes whether we could find the overlap region of TE and TM PBGs under the same structural parameters. To test this, a conventional triangular lattice PC slab was tried first, but the CPBG could not be obtained when the refractive index of the guided layer was lower than 3.5. Therefore, the choice of PC structure is important for obtaining CPBG in the lower RIC. Previous investigations have shown that both annular hole PCs [27, 28] and connecting-rods PCs [29–33] can increase the width of the 2D CPBGs. So here, a new PC formed by connecting annular holes (denoted as CAPC), as shown in the upper left corner of Fig. 1b, was proposed to inherit the features of previous two PCs. In Fig. 1b, r and R are the inner and outer radii of the annular hole, d represents the width of the connecting-rods, a is the lattice constant. Since CAPC has more adjustable parameters and greater degrees of freedom, the possibility of obtaining CPBGs should also be greater.

3 Optimization for complete photonic bandgap

In this stage of the work, optimization of structural parameters was performed to achieve a CPBG in the Si_xN_y CAPC slab. Firstly, as shown in Fig. 2b, within the whole single-mode frequency range, the effective index pairs (n_{TE}, n_{TM}) could be varied by changing the parameters b or λ. To obtain the maximum normalized CPBG, effective index pairs between single mode normalized frequencies 0.1718 and 0.3088 (b/λ) with a step size of 0.01 were chosen. Then, at each specific pair of n_{TE} and n_{TM}, the PBGs of TE and TM polarizations in the CAPC were calculated, respectively. Therefore, optimized parameters of planar structure in CAPC could be obtained. During the optimization, each of the three key structural parameters (d, r, R) was first scanned with a step of 0.01a, 0.025a, and 0.025a respectively, to obtain a preliminary view of the coincident frequency range of TE PBGs and TM PBGs under the same parameters. Then the parameter step of R and r was reduced to 0.005a for the structural parameter zones where CPBGs were located. Finally, as shown in Fig. 2a, when $n_{TE}=2.15$ and $n_{TM}=1.8$,

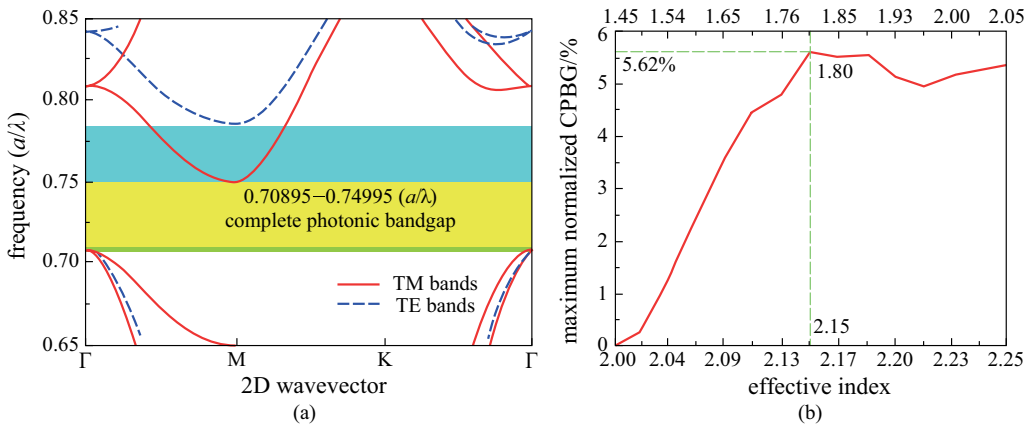

Fig. 2 **a** Band diagram of CAPC slab when $n_{TE}=2.15$ and $n_{TM}=1.8$, the corresponding structural parameters are $d=0.26a$, $r=0.3a$, and $R=0.4a$. The yellow shadow and blue shadow together denote the PBG for TE polarization (0.708953–0.785195 (a/λ)), the yellow shadow and green shadow together denote the PBG for TM polarization (0.707918–0.749946 (a/λ)), and the yellow shadow denotes the 2D slab PC CPBG (0.70895–0.74995 (a/λ)). **b** Maximum normalized CPBG of CAPC slab with different effective index pairs in the single-mode range, the lower axis represents the n_{TE}, and the upper axis represents the n_{TM}

the largest normalized CPBG of 5.62% was obtained for $d=0.26a$, $r=0.3a$, and $R=0.4a$.

Figure 2b shows the maximum normalized CPBG of the CAPC slab with different effective index pairs in the single-mode range. It can be clearly seen from Fig. 2b that, when n_{TE} within the range of 2.13–2.25 (corresponding to n_{TM} within the range of 1.76–2.05), relatively large CPBG could be maintained. However, when the n_{TE} is lower than 2.09 and n_{TM} is lower than 1.65, the size of CPBG begins to decrease sharply. Finally, when $n_{TE}=2$ and $n_{TM}=1.45$, CPBG disappears. The results indicate that CPBG is relatively stable within a certain wavelength or frequency range. Thus, in the whole single-mode frequency range, the largest normalized CPBG of 5.62% with $n_{TE}=2.15$ and $n_{TM}=1.8$ can be obtained. Moreover, as shown in Fig. 1a, for a wavelength of 1.55 μm, each frequency corresponds to a different thickness of the Si_xN_y slab. That means, in this frequency range where larger CPBGs are located, we can intentionally choose the Si_xN_y slab thickness within the fabrication limits. Considering for 1.55 μm wavelength, the structure parameters of the optimized CAPC slab with the largest normalized CPBG of 5.62% can all be designed: $b = 372$ nm, $d=293.96$ nm, $r=339.2$ nm, and $R=452.2$ nm, which should be possible to fabricate using state of the art technology [34, 35].

4 Microcavity structure based on the complete photonic bandgap

To further confirm how reliable the CPBG obtained in the triangular-lattice CAPC slab could be, as an example a dual-polarization microcavity was theoretically demonstrated by directly making use of the optimized CAPC slab with $n(Si_xN_y)=2.5$. We considered removing three CAPC in the middle to form a microcavity for the sake of simplicity, as shown in the upper left illustration in Fig. 3a. To study the light confinement of the microcavity, the effective index model which is the same as in Sect. 2, was considered. It should be clear that the microcavity could support both TE and TM modes. Figure 3a shows the quality factors of the resonance cavity modes as a function of the number of cells surrounding the defect, and when the number of cells is 14, the Q values of 197616 and 4968 have been obtained in the CAPC cavity for TE and TM resonance modes, respectively. Figure 3b shows the H_Z field for TE cavity mode having a Q value of 197616 with 14 cells, and Fig. 3c shows the E_Z field for TM cavity mode having a Q value of 4968 with 14 cells. Actually, during our investigation, we varied the number of the cells, from 10 to 20 with steps of 2. As shown in Fig. 3a, when increasing the number of cells, the Q value hugely increases due to existing CPBG of CAPC. This behavior has been explained in a photonic crystal book written by MIT [36]. In our investigation, the Q values were obtained by using the Harminv command in the MEEP software [37], accompanied by running very narrow-bandwidth point sources.

5 CPBG for Si_xN_y slab with other refractive indices

After the CPBG of CAPC slab with the RIC of 2.5 had been investigated, another question arose: could it be further extended to a Si_xN_y slab with lower RIC? Therefore,

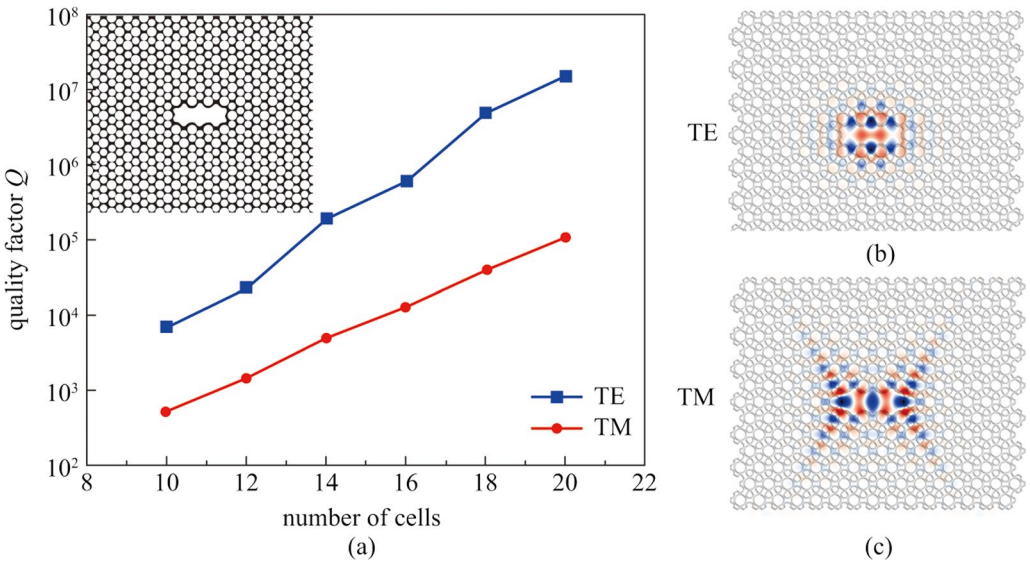

Fig. 3 **a** Quality factor of the CAPC cavity, the left upper shows schematic structures of microcavity with cells of 14. **b** H_Z field for TE cavity mode having a Q value of 197616 with 14 cells, the z direction is shown in the coordinate system in the lower right corner of Fig. 1a. **c** E_Z field for TM cavity mode having a Q value of 4968 with 14 cells, the z direction is shown in the coordinate system in the lower right corner of Fig. 1a

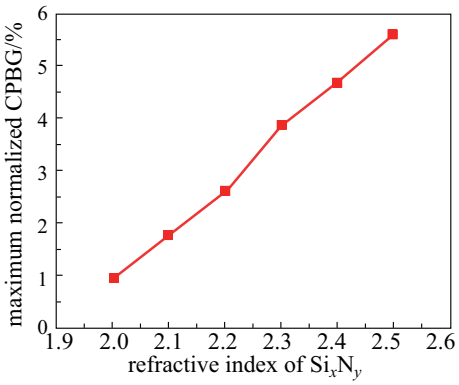

Fig. 4 Maximum normalized CPBG of CAPC slab with different refractive indices of Si_xN_y

based on the same method, we also calculated the CPBG of CAPC slab for Si_xN_y guided layer with other lower refractive indices.

It can be seen from Fig. 4 that as the refractive index of Si_xN_y decreases, the CPBG gradually becomes smaller. In other words, the size of the CPBG has a lot to do with the RIC of the material platform. More specifically, the higher the RIC of the material platform, the easier access is to CPBG, which leads to the higher possibility of TE PBGs and TM PBGs overlapping. Actually, the lowest refractive index of Si_xN_y for a CPBG can be extended to as low as 2. At this time, a normalized CPBG of 0.96% with $n_{TE}=1.8$ and $n_{TM}=1.67$ can be obtained, the corresponding structural parameters are $d=0.21a$, $r=0.25a$, $R=0.375a$.

6 Conclusions

In conclusion, by utilizing the difference between effective index of TE polarization and TM polarization, large normalized CPBG of 5.62% can be obtained in the 2D Si_xN_y slab consisting of triangular-lattice CAPC. The investigation indicates that both the method of using effective index difference between TE and TM polarizations and the structure of CAPC are essential for obtaining a large CPBG in the lower RIC. The method is a prerequisite or offers a shortcut for engineering a suitable PC structure to obtain a large CPBG. However, if the method is not compatible with a good performance structure, the effect may not be beneficial. Therefore, the adoption of CAPC is also crucial.

Moreover, a microcavity which could support both TE and TM polarization in the CAPC slab was theoretically demonstrated by making use of the optimized CPBG. Both H_Z field and E_Z field could show that the microcavity has good performance in confining light, which demonstrated the reliability of the CPBG obtained in the triangular-lattice CAPC slab. Based on our study as reported in this paper, other useful applications like polarization-independent waveguide devices can also be suitably designed. Furthermore, the CPBG of CAPC slab for Si_xN_y with other refractive indices was also performed. We noticed that the CPBG of the Si_xN_y slab could remain existing until a record low index contrast of 2 in this work. The result indicates that development of high-performance CPBG devices in Si_xN_y slab would be possible. It also provides encouragement that there may be significant improvements remaining to be discovered in designing and optimizing silicon based CPBG devices.

Acknowledgements This work was supported by the National Natural Science Foundation of China (Grant Nos. 11504435 and 62171478), and the Natural Science Foundation of Hubei Province, China (No. 2020CFB450).

Author contributions CM carried out the research of complete photonic bandgap in silicon nitride slab, performed the data analyses and drafted some part of the manuscript; JH provided the conception of the study, contributed significantly to the analysis and manuscript preparation, and wrote some part of the manuscript; CY, MS, and SC helped perform the analysis with constructive discussions and wrote some part of the manuscript. All authors read and approved the final manuscript.

Declarations

Competing interests The authors declare that they have no competing interests.

References

1. Akahane, Y., Asano, T., Song, B.S., Noda, S.: High-*Q* photonic nanocavity in a two-dimensional photonic crystal. Nature **425**(6961), 944–947 (2003)
2. Morita, Y., Tsuji, Y., Hirayama, K.: Proposal for a compact resonant-coupling-type polarization splitter based on photonic crystal waveguide with absolute photonic bandgap. IEEE Photonics Technol. Lett. **20**(2), 93–95 (2008)
3. Guo, H.M., Hong, X.R., Fan, H.R., Fu, R., Liu, X., Li, Y.X., Feng, S., Chen, X., Li, C.B., Wang, Y.Q.: Polarization-independent waveguides based on the complete band gap of the two-dimensional photonic crystal slabs. Laser Phys. **29**(4), 046205 (2019)
4. Turduev, M., Giden, I.H., Kurt, H.: Modified annular photonic crystals with enhanced dispersion relations: polarization

insensitive self-collimation and nanophotonic wire waveguide designs. J. Opt. Soc. Am. B Opt. Phys. **29**(7), 1589–1598 (2012)
5. Tsuji, Y., Morita, Y., Hirayama, K.: Photonic crystal waveguide based on 2-D photonic crystal with absolute photonic band gap. IEEE Photonics Technol. Lett. **18**(22), 2410–2412 (2006)
6. Kalra, Y., Sinha, R.K.: Design of ultra compact polarization splitter based on the complete photonic band gap. Opt. Quant. Electron. **37**(9), 889–895 (2005)
7. Wen, F., David, S., Checoury, X., El Kurdi, M., Boucaud, P.: Two-dimensional photonic crystals with large complete photonic band gaps in both TE and TM polarizations. Opt. Express **16**(16), 12278–12289 (2008)
8. Bayer, C., Straub, M.: Small-hole waveguides in silicon photonic crystal slabs: efficient use of the complete photonic bandgap. Appl. Opt. **48**(27), 5050–5054 (2009)
9. Wu, H., Citrin, D.S., Jiang, L., Li, X.: Polarization-independent single-mode waveguiding with honeycomb photonic crystals. IEEE Photonics Technol. Lett. **27**(8), 840–843 (2015)
10. Jalali, B.: Nonlinear optics in the mid-infrared. Nat. Photonics **4**(8), 506–508 (2010)
11. Tan, D.T.H., Ooi, K.J.A., Ng, D.K.T.: Nonlinear optics on silicon-rich nitride—a high nonlinear figure of merit CMOS platform. Photonics Res. **6**(5), B50 (2018)
12. Moss, D.J., Morandotti, R., Gaeta, A.L., Lipson, M.: New CMOS-compatible platforms based on silicon nitride and Hydex for nonlinear optics. Nat. Photonics **7**(8), 597–607 (2013)
13. Matsushita, S., Suavet, O., Hashiba, H.: Full-photonic-bandgap structures for prospective dye-sensitized solar cells. Electrochim. Acta **55**(7), 2398–2403 (2010)
14. Matsushita, S., Matsutani, A., Morii, Y., Kobayashi, D., Nishioka, K., Shoji, D., Sato, M., Tatsuma, T., Sannomiya, T., Isobe, T., Nakajima, A.: Calculation and fabrication of two-dimensional complete photonic bandgap structures composed of rutile TiO_2 single crystals in air/liquid. J. Mater. Sci. **51**(2), 1066–1073 (2016)
15. Spurny, M., O'Faolain, L., Bulla, D.A.P., Luther-Davies, B., Krauss, T.F.: Fabrication of low loss dispersion engineered chalcogenide photonic crystals. Opt. Express **19**(3), 1991–1996 (2011)
16. Suzuki, K., Baba, T.: Nonlinear light propagation in chalcogenide photonic crystal slow light waveguides. Opt. Express **18**(25), 26675–26685 (2010)
17. Grillet, C., Smith, C., Freeman, D., Madden, S., Luther-Davies, B., Magi, E., Moss, D., Eggleton, B.: Efficient coupling to chalcogenide glass photonic crystal waveguides via silica optical fiber nanowires. Opt. Express **14**(3), 1070–1078 (2006)
18. Cerjan, A., Fan, S.H.: Complete photonic band gaps in supercell photonic crystals. Phys. Rev. A **96**(5), 051802 (2017)
19. Rahim, A., Ryckeboer, E., Subramanian, A.Z., Clemmen, S., Kuyken, B., Dhakal, A., Raza, A., Hermans, A., Muneeb, M., Dhoore, S., Li, Y., Dave, U., Bienstman, P., Le Thomas, N., Roelkens, G., Van Thourhout, D., Helin, P., Severi, S., Rottenberg, X., Baets, R.: Expanding the silicon photonics portfolio with silicon nitride photonic integrated circuits. J. Lightwave Technol. **35**(4), 639–649 (2017)
20. Lacava, C., Stankovic, S., Khokhar, A.Z., Bucio, T.D., Gardes, F.Y., Reed, G.T., Richardson, D.J., Petropoulos, P.: Si-rich silicon nitride for nonlinear signal processing applications. Sci. Rep. **7**(1), 22 (2017)
21. Ooi, K.J., Ng, D.K., Wang, T., Chee, A.K., Ng, S.K., Wang, Q., Ang, L.K., Agarwal, A.M., Kimerling, L.C., Tan, D.T.: Pushing the limits of CMOS optical parametric amplifiers with USRN:Si_7N_3 above the two-photon absorption edge. Nat. Commun. **8**, 13878 (2017)
22. Kawano, K.K.T.: Introduction to Optical Waveguide Analysis: Solving Maxwell's Equations and the Schrödinger Equation. Wiley, Hoboken (2002)
23. Qiu, M.: Effective index method for heterostructure-slab-waveguide-based two-dimensional photonic crystals. Appl. Phys. Lett. **81**(7), 1163–1165 (2002)
24. Qiu, M., Azizi, K., Karlsson, A., Swillo, M., Jaskorzynska, B.: Numerical studies of mode gaps and coupling efficiency for line-defect waveguides in two-dimensional photonic crystals. Phys. Rev. B **64**(15), 155113 (2001)
25. Hou, J., Citrin, D.S., Cao, Z., Yang, C., Zhong, Z., Chen, S.: Slow light in square-lattice chalcogenide photonic crystal holey fibers. IEEE J. Sel. Top. Quantum Electron. **22**(2), 271–278 (2016)
26. Johnson, S., Joannopoulos, J.: Block-iterative frequency-domain methods for Maxwell's equations in a planewave basis. Opt. Express **8**(3), 173–190 (2001)
27. Rezaei, B., Fathollahi Khalkhali, T., Soltani Vala, A., Kalafi, M.: Absolute band gap properties in two-dimensional photonic crystals composed of air rings in anisotropic tellurium background. Opt. Commun. **282**(14), 2861–2869 (2009)
28. Proietti Zaccaria, R., Verma, P., Kawaguchi, S., Shoji, S., Kawata, S.: Manipulating full photonic band gaps in two dimensional birefringent photonic crystals. Opt. Express **16**(19), 14812–14820 (2008)
29. Chau, Y.F., Wu, F.L., Jiang, Z.H., Li, H.Y.: Evolution of the complete photonic bandgap of two-dimensional photonic crystal. Opt. Express **19**(6), 4862–4867 (2011)
30. Giden, I.H., Kurt, H.: Modified annular photonic crystals for enhanced band gap properties and iso-frequency contour engineering. Appl. Opt. **51**(9), 1287–1296 (2012)
31. Ma, T.X., Wang, Y.S., Zhang, C.: Investigation of dual photonic and phononic bandgaps in two-dimensional phoxonic crystals with veins. Opt. Commun. **312**, 68–72 (2014)
32. Shi, P., Huang, K., Li, Y.: Photonic crystal with complex unit cell for large complete band gap. Opt. Commun. **285**(13–14), 3128–3132 (2012)
33. Wang, Y.F., Wang, Y.S., Su, X.X.: Large bandgaps of two-dimensional phononic crystals with cross-like holes. J. Appl. Phys. **110**(11), 113520 (2011)
34. Luke, K., Dutt, A., Poitras, C.B., Lipson, M.: Overcoming Si_3N_4 film stress limitations for high quality factor ring resonators. Opt. Express **21**(19), 22829–22833 (2013)
35. Tan, D.T.H., Ikeda, K., Sun, P.C., Fainman, Y.: Group velocity dispersion and self phase modulation in silicon nitride waveguides. Appl. Phys. Lett. **96**(6), 061101 (2010)
36. Joannopoulos, J.D., Winn, J.N., Meade, R.D.: Photonic Crystal Molding the Flow of Light, 2nd edn. Princeton University, New Jersey (2008)
37. Oskooi, A.F., Roundy, D., Ibanescu, M., Bermel, P., Joannopoulos, J.D., Johnson, S.G.: MEEP: a flexible free-software package for electromagnetic simulations by the FDTD method. Comput. Phys. Commun. **181**(3), 687–702 (2010)

Can Ma received the bachelor degree in Communication Engineering in June 2019, from Electronic and Information Engineering, South-Central MinZu University, China. She is currently pursuing the master degree in Optical Engineering there. Her present research work involves optical communication and integrated optical devices.

Jin Hou received the B.S. degree in Thermal Power Engineering in June 2003 from Harbin University of Science and Technology, China, the M.S. degree in instrument science and technology in June 2006 from Harbin Institute of Technology, China, and the Ph.D. degree in Optoelectronic Information Engineering from Huazhong University of Science and Technology, China. He was also a Visiting Scholar in Prof. David S. Citrin's research group, Georgia Tech, USA, from December 2009 to March 2011 and from December 2018 to December 2019. From June 2011, he joined College of Electronics and Information Engineering, South-Central MinZu University (Wuhan, China) as an Assistant Professor. In June 2013, he was promoted to an Associate Professor. Since January 2019, he has been a Professor there. He has served as a reviewer for publications such as *Optics Express*, *Applied Optics*, *IEEE Journal of Selected topics in Quantum Electronics*, and *IEEE Photonics Journal*. In recent years, more than 40 academic papers have been published. His current research interests include silicon-based optoelectronics, optical fiber and optical communication, intelligent detection and signal processing.

Chunyong Yang received the B.S. degree in Electrical Engineering from Central China Normal University, China, in 1998. Then he studied in the graduate school of University of Science and Technology of China, China, in 1999, and received the M.S. degree in Electrical Engineering from Institute of Seismology, China Earthquake Administration, China, in 2001, and the Ph.D. degree in Electronics Engineering from Huazhong University of Science and Technology, China, in 2005. From 2005 to 2013, he was an Assistant Professor and an Associate Professor with College of Electronics and Information Engineering, South-Central MinZu University, China, where he is currently a Professor. In 2017, he was selected into the national talent pool of ten thousand outstanding innovation and entrepreneurship tutors. In 2019, he was selected into the Young Talents Program of the National Ethnic Affairs Commission. He serves as a reviewer for publications such as *Optics Express*, *Applied Optics*, *Optics Communications*, and *IEEE Photonics Journal*. In recent years, more than 40 academic papers have been published. His research interests include optical communication and optical sensing, optoelectronic fusion communication, intelligent perception and detection.

Ming Shi received the B.S. degree from School of Physical Engineering, Zhengzhou University, China, and the Ph.D. degree from Shanghai Institute of Technical Physics, Chinese Academy of Sciences, China. He is currently an associate professor at College of Electronic Information Engineering, South-Central MinZu University, China. His current research interests include intelligent optical communication and photoelectric detection.

Shaoping Chen received the B.S. and M.S. degrees from Wuhan University, China, in 1987 and 1990, respectively, both in Electrical Engineering, and the Ph.D. degree in Information and Communication Engineering from Huazhong University of Science and Technology, China, in 2004. He joined College of Electronics and Information Engineering, South-Central MinZu University, China, in 1990. Now he is the deputy director of the Academic Committee of the South-Central MinZu University, the director of the Hubei Key Laboratory of Intelligent Wireless Communications, the member of the Academic Committee of the National Green Communication and Network International Joint Center, and the editor of "Chinese Journal on Internet of Things" Committee. He got Second Class of Hubei Natural Science Award twice, separately in 2011 and 2018. In 2019, he was awarded as the Outstanding Contribution Expert of the National Ethnic Affairs Commission. His research interests include the communication theory, wireless and optical communication systems, Internet of Things technology and its applications.